Enhanced Multiplexing Capacity of Low-Coherence Reflectometric Sensors With a Loop Topology

Libo Yuan, Wei Jin, Limin Zhou, Y. L. Hoo, and M. S. Demokan

***Abstract*—A novel scheme for enhancing the multiplexing capacity of low-coherence reflectometric sensors is demonstrated. The scheme is based on connecting the sensing elements in serial in a loop configuration, allowing each of the sensors within the array being interrogated twice from opposite directions. The bi-directional interrogation enhances the multiplexing capacity in terms of maximum sensor number. The bi-interrogation scheme would also allow normal operation of the sensor array even when one end or somewhere of the transmission fiber were broken, improving the reliability of the sensing system for large-scale structural monitoring.**

***Index Terms*—Fiber-optic sensors, low-coherence reflectometry, quasidistributed sensors, strain sensors.**

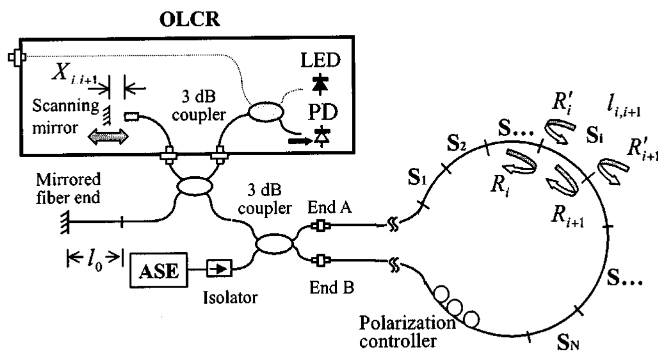

Fig. 1. Schematic of the multiplexing scheme based on the loop topology.

I. INTRODUCTION

OPTICAL low-coherence reflectometry (OLCR) [1], [2] has emerged as high-resolution measurement technique for optical device testing [3]–[6]. OCLR is based on the use of a low coherence light source and a scanning optical (Michelson) interferometer to match the optical paths of the reflected waves from the device under test. OCRL has been applied for quasidistributed sensing [7]–[14] by intentionally introducing partial reflectors along an optical fiber. The gauge lengths of the sensors (defined between two partial reflectors) are chosen to be longer than the coherence length of the source so that the reflected waves from the two end-faces of a sensing gauge would not mix coherently before they reach the scanning interferometer. An interferogram appears at the output of the scanning interferometer only when its optical path difference (OPD) is matched to the gauge length of a particular sensor. A series of interferometric maximums or peaks are resulted when the OPD of the interferometer is scanned through all the possible gauge lengths of the sensors. The positions of the peaks can then be used as measures of the gauge lengths of the sensors.

This letter reports a scheme that can enhance the multiplexing capacity of low-coherence reflectometric sensors. The scheme offers larger multiplexing gain, higher reliability over the conventional reflectometry sensor array. The higher reliability is achieved through the use of bi-directional interrogation of each sensor in the array, which provides an extra degree of redundancy and is important for embedded applications in large-scale smart structures.

Manuscript received January 29, 2002; revised April 26, 2002. This work was supported in part by the National Natural Science Foundation of China under Grant Number 50179007, by the Science Foundation of Heilongjiang Province for Outstanding Youth, 1999 to the Harbin Engineering University, and by the Hong Kong Polytechnic University under Grant G-W099 and Grant G-YC64.

L. Yuan is with the Department of Physics, Harbin Engineering University, Harbin 150001, China (e-mail: lbyuan@vip.sina.com) and also with the Department of Mechanical Engineering, The Hong Kong Polytechnic University, Hong Kong, China.

W. Jin, Y. L. Hoo, and M. S. Demokan are with the Department of Electrical Engineering, The Hong Kong Polytechnic University, Hong Kong, China.

L. Zhou is with the Department of Mechanical Engineering, The Hong Kong Polytechnic University, Hong Kong, China.

Publisher Item Identifier S 1041-1135(02)06261-4.

II. DESCRIPTION OF THE SCHEME

The proposed multiplexing scheme is shown in Fig. 1. Light from a low coherence source (an Er-doped ASE source is shown in Fig. 1) is coupled into a fiber Sagnac loop through a 3 dB coupler. The fiber loop contains a serially connected sensor array $S_1, S_2, \ldots, S_N$, with each one of them $(S_i, i = 1, 2, \ldots, N)$ being formed in-between two partial reflectors i and $i + 1$. The gauge lengths of the sensors (denoted as $l_{i,i+1}$ for S_i) are chosen to be approximately equal but slightly different from each other. There are four reflected waves from the two ends of the sensor S_i, two reflected back toward end A clockwise (CW) and the other two toward end B counterclockwise (CCW). The four waves are guided back through the 3-dB coupler to a Michelson interferometer with its output monitored by a photodetector (PD). The optical path difference (OPD) of the interferometer is set to be approximately equal to the sensor gauge length ($l_0 \approx l_{i,i+1}$ for $i = 1, 2, \ldots, N$) and can be varied through the use of a scanning mirror as shown in Fig. 1.

In Fig. 1, the light-emitting diode and the part with dotted line are not used. The components within the OLCR box are part of a commercial precision reflectometer (HP8504B). We here use only the scanning mirror and the photodetector within the box. As the scanning mirror moving on the translation stage, there will be N groups of interference fringes appear, which corresponding to the OPD of the interferometer matched to that of the N sensors in the loop. The peak fringe intensity at the photo-detector corresponds to the ith sensor, which is due to the coherent mixing between the reflected waves from the ith and the $(i+1)$th reflectors, may be expressed as (See the equation at the bottom of the page.) Where I_0 represents the light intensity coupled into the input optical fiber from the ASE source. The insertion losses of the 3-dB coupler has been neglected. β_i and β_i' represent, respectively, the excess losses associated with sensor S_i, which is due to the connection loss between the sensing segments, for the CW and the CCW propagating light waves. $T_i(T_i')$ and $R_i(R_i')$ are respectively the transmission and reflection coefficient of the ith partial reflector. $T_i(T_i')$ is in general smaller than $1-R_i$ $(1-R_i')$ because of the loss factor $\beta_i(\beta_i')$. The values of T_i, R_i and β_i could be different from that of T_i', R_i', and β_i'. $\eta(X_{i,i+1})$ is the loss associated with the scanning mirror and collimating optics and is a function of the scanning mirror position $X_{i,i+1}$. R_f and R_m are the reflectivities of the mirrored fiber end and the scanning mirror, respectively.

III. Experiments and Results

Experiments were conducted using a setup shown in Fig. 1. An Er-doped fiber amplified spontaneous emission (ASE) source with a central wavelength around 1.55 μm was used in our experiment. The source emits unpolarized light with power level adjustable from 0–10 mW. Ten segments of sensing fiber, each with a length of approximately 1-m were cleaved and then connected (butt-coupled) in serial to form the sensing array. The gauge length differences between the adjacent sensors were chosen to be about 10 mm. The output from the scanning Michelson interferometer was displayed on the screen of the precision reflectometer instrument. A typical display is shown in Fig. 2 for a source power level of -4.63 dBm (0.34 mW). The results shown in Fig. 2(a) and (b) are respectively for the cases where the loop was closed and open at end A. The heights of the peaks in Fig. 3(a) and (b) are irregular because that it is difficult to ensure the reflectivity of each of the fiber segment is the same.

It can be seen that the results shown in Fig. 2(a) and (b) essentially provide the same measurement information in terms of the positions of the peaks. This means that the system would function the same even one end of the loop is disconnected. The signal level for the closed loop case is however higher than the open loop case. For the particular light level of -4.63 dBm, the signal level for sensor #1 may be too small for the accurate measurement of the peak position when the loop is open at end A [Fig. 2(b)], similarly, open at end B due to the symmetry of the loop architecture. The signal level was significantly enhanced when the loop was closed [Fig. 2(a)]. This means that, for the same source power level, the maximum sensor number can be increased with the closed loop configuration.

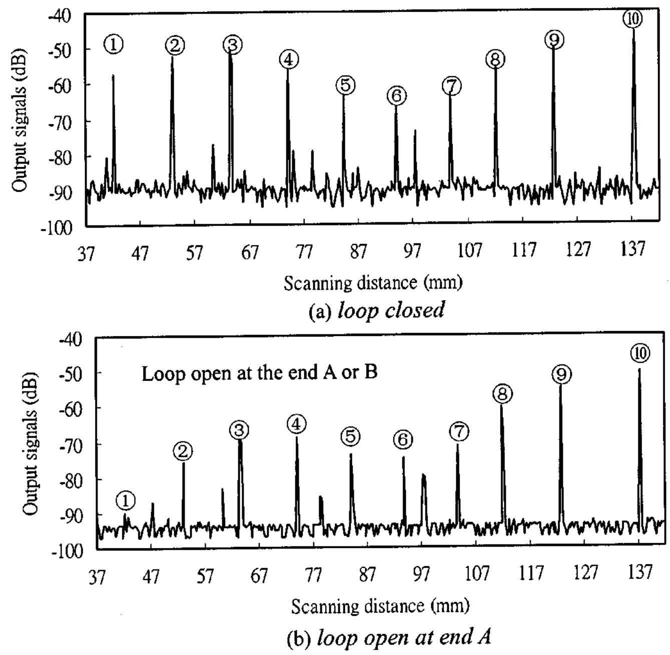

Fig. 2. Output from the ten fiber-optic sensor array with input power level $= -4.63$ dBm.

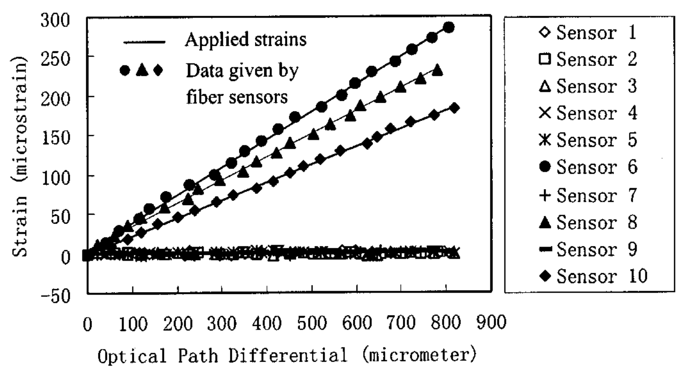

Fig. 3. Distributed strain measurement results.

In order to demonstrate the applicability of the system in real distributed deformation or strain measurements. Strains are applied on 6th, 8th, and 10th fiber-optic sensors, and let the other seven sensors in free state. The testing results are plotted in Fig. 3, it is shown that the fiber optic sensors connected in the fiber loop can mapping the applied strain conditions, while the 7 sensors did not perturbed and its interference pattern peak positions almost have not any shift. The resolution of the strain sensing system is 6 $\mu\varepsilon$ for present 1-m fiber gauge length case, and the measuring accuracy is 10 $\mu\varepsilon$.

$$I_D(i,i+1) = \frac{I_0}{16}\sqrt{R_f R_m \eta(X_{i,i+1})}\left\{\begin{array}{c} \left[\prod_{k=1}^{i-1} T_k\beta_k\right]\left[\prod_{k=1}^{i-1} T_k'\beta_k'\right]\sqrt{R_i R_{i+1} T_i \beta_i T_i' \beta_i'} \\ + \\ \left[\prod_{k=i+2}^{N+1} T_k'\beta_k'\right]\left[\prod_{k=i+2}^{N+1} T_k\beta_k\right]\sqrt{R_i' R_{i+1}' T_{i+1}' \beta_{i+1}' T_{i+1}\beta_{i+1}} \end{array}\right\}$$

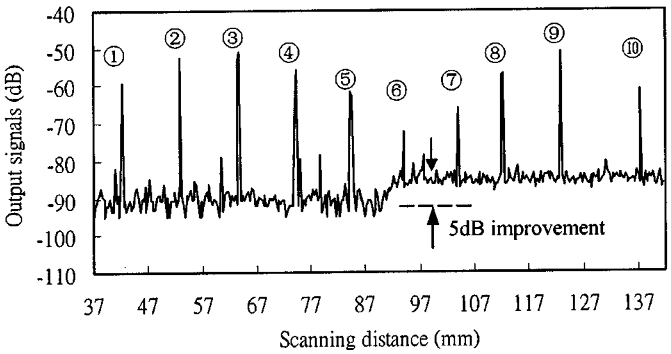

Fig. 4. A 5-dB reduction in the noise floor is achieved by adjusting the polarization stages.

IV. DISCUSSIONS

It should be mentioned that, although the measurement results for a linear array with loop open at either end A or B is polarization independent (in the strict sense, the effect of polarization is neglected in that case), the results obtained from the closed loop measurements are dependent on the polarization states. Fig. 4 shows the variation of the signals when the polarization controller in the loop (see Fig. 1) was adjusted. This is because light signals that are not reflected at the partial reflectors (transmitted) would mix coherently at the loop coupler as they traveled through the optical path length. When the counterpropagating (transmitted) light signals are of the same polarization states, the light signal at the output port of the loop would approach zero due to destructive interference [15]. When the counterpropagating signals are of different polarization, the orthogonal polarization components would add up in intensity and result in a noise floor. And as the variation of deformation in each gauge length of the sensor starting from the first sensor would change the state of polarization. In that case, their multisensing capability would have been reduced. It may therefore necessary to control the polarization states in order to achieve the optimal results. One method is by way of insert a depolarizer between the ASE light source and the 3-dB coupler, the other solution is using polarization maintain fiber in the sensing system to over come the unstable of polarization state.

The disadvantage of the loop topology scheme is also obvious, such as the need for access to both fiber ends which leading to more complicated fiber-optic sensors installation.

V. SUMMARY

A novel scheme for enhancing the multiplexing capacity of low coherence reflectometric sensors was demonstrated. The scheme is based on the bidirectional interrogation of the sensors in the array using a loop topology. For the same source power level, this scheme doubles the multiplexing gain in terms of maximum sensor number. The scheme has the same accuracy in the determination of the positions of the interferometric peaks, but would allow normal operation the sensor array even when a point in the sensing array is broken, offering additional redundancy, which is often required for the monitoring of large structures. The sensor array is completely passive and can be used to perform absolute, quasi-distributed deformation measurements, or quasi-distributed strain or temperature measurements.

REFERENCES

[1] R. C. Younquist, S. Catt, and D. E. N. Davies, "Optical coherence-domain reflectometry: A new optical evaluation technique," *Opt. Lett.*, vol. 12, pp. 158–160, 1987.
[2] B. L. Danielson and C. D. Whittenberg, "Guided-wave reflectometry with micrometer resolution," *Appl. Opt.*, vol. 26, p. 2836, 1987.
[3] K. Takada, I. Yokohama, K. Chida, and J. Noda, "New measurement system for fault location in optical waveguide devices based on an interferometric technique," *Appl. Opt.*, vol. 26, p. 1603, 1987.
[4] L. Thevenaz, J. P. Pellaux, and J. P. von der Weid, "All-fiber interferometer for chromatic dispersion measurements," *J. Lightwave Technol.*, vol. 6, pp. 1–7, Jan. 1988.
[5] K. Takada, K. Yukimatsu, M. Kobayashi, and J. Noda, *Appl. Phys. Leet.*, vol. 59, p. 143, 1991.
[6] X. Clivaz, F. Marquis-Weible, R. P. Salathe, R. P. Novak, and H. H. Gilgen, "High-resolution reflectometry in biological tissues," *Opt. Lett.*, vol. 17, pp. 4–6, 1992.
[7] S. A. Al-Chalabi, B. Culshaw, and D. E. N. Davies, "Partially coherent sources in interferometry," in *IEE Proc. 1st Int. Conf. Optical Fiber Sensors*, London, U.K., 1983, pp. 132–135.
[8] J. L. Brooks, R. H. Wentworth, R. C. Youngquist, M. Tur, B. Y. Kim, and H. J. Shaw, "Coherence multiplexing of fiber optic interferometric sensors," *J. Lightwave Technol.*, vol. 3, pp. 1062–1071, 1985.
[9] A. B. L. Ribeiro and D. A. Jackson, "Low coherence fiber optic system for remote sensors illuminated by a 1.3 μm multimode laser diode," *Rev. Sci. Instrum.*, vol. 64, pp. 2974–2977, 1993.
[10] D. Inaudi, A. Elamari, L. Pflug, N. Gisin, J. Breguet, and S. Vurpillot, "Low-coherence deformation sensors for the mornitoring of civil-engineering structures," *Sensors and Actuators A*, vol. 44, pp. 125–130, 1994.
[11] W. V. Sorin and D. M. Baney, "Multiplexing sensing using optical low-coherence reflectometry," *IEEE Photon. Technol. Lett.*, vol. 7, pp. 917–919, Aug. 1995.
[12] L. B. Yuan and F. Ansari, "White light interferometric fiber-optic distributed strain-sensing system," *Sensors and Actuators: A*, vol. 63, pp. 177–181, 1997.
[13] L. B. Yuan and L. Zhou, "1 $\times$ N star coupler as distributed fiber optic strain sensor using in white light interferometer," *Appl. Opt.*, vol. 37, pp. 4168–4172, 1998.
[14] L. B. Yuan, L. Zhou, and W. Jin, "Quasidistributed strain sensing with white-light interferometry: A novel approach," *Opt. Lett.*, vol. 25, pp. 1074–1076, 2000.
[15] W. Jin, "Fiber optic gyroscope," in *Guided Wave Optical Sensors*, W. Jin, Y. Liao, and Z. Zhang, Eds. Beijing, China: Science Press, 1998, pp. 148–176.